

### Summary

A novel, redox-active cryptand containing an anthraquinone group has been studied by cyclic voltammetric and ESR techniques in the presence and absence of  $\text{Li}^+$ ,  $\text{Na}^+$ , and  $\text{K}^+$  cations. An unexpected 1:2 ( $\text{L}^{\cdot-}:\text{2Li}^+$ ) symmetric complex was easily detected by ESR spectroscopy, even when the relative stoichiometric ratio present was only 1:1. The presence of such a complex was confirmed using cyclic voltammetry and alkali-metal NMR (both  $^{23}\text{Na}$  and  $^7\text{Li}$ ). The voltammetric results show, for the first time, the direct resolution of six reduction waves, two for each of the ligand states. These are the free ligand, the 1:1 complex, and the 1:2 complex. Previously, a maximum of only four resolved reductions had been observed for an anthraquinone podand.<sup>5</sup> The structure of this 1:2 complex probably involves an interaction of the two  $\text{Li}^+$  cations with the anthraquinone carbonyl that points to the inside of the cryptand cavity. Based on CPK models, it is possible for the two cations to each "sit" comfortably on two "pockets" created by the crown around this carbonyl. This proposal is structurally in accord with previous ESR observations involving **4**, which showed that two  $\text{Na}^+$  can interact with the same carbonyl while being enveloped by two podand side arms.

ESR and voltammetry also provide evidence for 1:2 complexes between  $\text{2}^{\cdot-}$  and  $\text{Na}^+$  or  $\text{K}^+$ . ESR spectral changes associated with 1:2 complex formation include increased line broadening and redistribution of spin density, as reflected by hydrogen coupling constant differences. On the other hand, it was not possible to

resolve more than one metal cation nuclear splitting as in the case with  $\text{Li}^+$ . These observations have been interpreted in terms of a 1:2 complex where one of the  $\text{M}^+$  is cryptated and the other one is interacting with the external carbonyl on the anthraquinone. The latter is probably in fast exchange with the solvent; thus, it is not possible to resolve its splitting, but it can lead to appreciable line broadening. Such 1:2 complexes were detected by cyclic voltammetry as well. For the 1:1 complex of the anion radical with  $\text{K}^+$ , it was not possible to return the ESR spectrum back to that of the free anion radical upon addition of cryptand [2.2.2]. This indicates that the complex formed by  $\text{2}^{\cdot-}:\text{K}^+$  is at least as strong as that formed by [2.2.2]: $\text{K}^+$ .

**Acknowledgment.** We thank the National Institutes of Health for Grant GM 33940 which supported this work. We wish to also thank the National Science Foundation, Division of Chemistry Grant No. CHE-9011901, for partial support. We also thank Dr. Rosario Concepcion for simulating the ESR spectrum for the species with sodium.

**Registry No.** **2**, 137571-97-2;  $\text{2}^{\cdot-}$ , 137571-98-3;  $\text{2}^{\cdot-}:\text{2Li}^+$ , 137572-00-0;  $\text{2}^{\cdot-}:\text{2Na}^+$ , 137572-01-1;  $\text{2}^{\cdot-}:\text{2K}^+$ , 137572-02-2;  $\text{2}^{\cdot-}:\text{Li}^+$ , 137572-03-3;  $\text{2}^{\cdot-}:\text{Na}^+$ , 137572-04-4;  $\text{2}^{\cdot-}:\text{K}^+$ , 137572-05-5;  $\text{2}^{\cdot-}$ , 137571-99-4; **4**, 13-diaza-18-crown-6, 23978-55-4; 1,8-bis(2-bromoethoxy)anthraquinone, 69595-68-2; 1,8-dihydroxyanthraquinone, 117-10-2; cryptand[2.2.2]: $\text{Na}^+$ , 32611-94-2; cryptand[2.2.2]: $\text{K}^+$ , 61624-59-7; cryptand[2.2.2]: $\text{Ag}^+$ , 57692-62-3.

## In Situ Atomic Force Microscopy of Underpotential Deposition of Ag on Au(111)

Chun-hsien Chen, Scott M. Vesecky, and Andrew A. Gewirth\*

Contribution from the Department of Chemistry, University of Illinois, 505 South Mathews Avenue, Urbana, Illinois 61801. Received August 8, 1991

**Abstract:** Atom-resolved atomic force microscope (AFM) images of underpotentially deposited (upd) monolayers of Ag on Au(111) are presented. These images show that the structure of this monolayer is dependent on the nature of the electrolyte in which the upd process occurs. Specifically, Ag shows a  $3 \times 3$  overlayer in sulfuric acid and a  $4 \times 4$  overlayer in nitrate- and carbonate-containing electrolytes. In perchloric acid a more complex structure is observed which, like the sulfate and nitrate systems, is also not close packed. In acetate, a close-packed monolayer is formed. The different monolayer structures give rise to packing densities which correlate with electrolyte size, except in the case of perchloric acid. However, there is little agreement between packing densities predicted from coulometric measurements and those actually observed with the AFM. The discrepancy between the two measurements is ascribed to differing amounts of charge transfer between electrolyte and adatom which alters the amount of charge needed for upd lattice formation.

### 1. Introduction

The focus of electrochemical surface science is correlation of electrode surface structure with electrochemical reactivity. Much attention in this area has centered on the underpotential deposition (upd) process,<sup>1-3</sup> in which a monolayer or submonolayer of a foreign metal adatom is deposited at potentials positive from the reversible Nernst potential. Upd can be thought of as the formation of a substrate-adatom bond before the formation of a somewhat weaker adatom-adatom bond during bulk deposition. The monolayers formed during the upd process are interesting not only because of their physical properties which are different from bulk phases of either the surface or the adatom, but also because they exhibit catalytic activity toward the electrooxidation of small organic molecules.

A central focus of studies of the upd process is the structure of the metal adsorbate on the surface. While this aspect has been

addressed extensively via both in situ and ex situ methods, direct confirmation of the monolayer structure has been elusive. Scanning tunneling microscope (STM) measurements<sup>4</sup> have provided substantial new information about upd,<sup>5</sup> but atomic resolution has been achieved in only a few upd systems.<sup>6-8</sup>

(1) Kolb, D. M. In *Advances in Electrochemistry and Electrochemical Engineering*; Gerischer, H., Tobias, C. W., Eds.; Wiley-Interscience: New York, 1978; Vol. 11, pp 125-271.

(2) Adzic, R. In *Advances in Electrochemistry and Electrochemical Engineering*; Gerischer, H., Tobias, C. W., Eds.; Wiley-Interscience: New York, 1984; Vol. 13, pp 159-260.

(3) Juttner, K.; Lorenz, W. J. *Phys. Chem. (Wiesbaden)* **1980**, *122*, 163.

(4) Reviews: (a) Sonnenfeld, R.; Schneir, J.; Hansma, P. K. In *Modern Aspects of Electrochemistry*; White, R. E., Bockris, J. O'M., Conway, B. E., Eds.; Plenum: New York, 1990; Vol. 21, pp 1-28. (b) Cataldi, T. R. I.; Blackham, I. G.; Briggs, G. A. D.; Pethica, J. B.; Hill, H. A. O. *J. Electroanal. Chem. Interfacial Electrochem.* **1990**, *290*, 1-20.

(5) (a) Green, M. P.; Hanson, K. J.; Carr, R.; Lindau, I. *J. Electrochem. Soc.* **1990**, *137*, 3493-3498. (b) Green, M. P.; Hanson, K. J.; Scherson, D. A.; Xing, X.; Richter, M.; Ross, P. N.; Carr, R.; Lindau, I. *J. Phys. Chem.* **1989**, *93*, 2181-2184.

\* To whom correspondence should be addressed.

However, following the demonstration<sup>9</sup> that the atomic force microscope<sup>10</sup> (AFM) could image metal surfaces immersed in liquid, we<sup>11,12</sup> showed that the AFM could be used to investigate electrochemical processes in situ with atomic resolution. We focused on the underpotential deposition of Cu on Au(111) and demonstrated in situ that the structure of the first upd monolayer was dependent on the electrolyte. Specifically, we showed that upd of Cu on Au(111) in sulfate led to a  $\sqrt{3}\times\sqrt{3}R30^\circ$  structure while in perchlorate the monolayer was close packed and incommensurate with the underlying Au(111). This behavior has also been seen in ex situ studies.<sup>13</sup> The  $\sqrt{3}\times\sqrt{3}R30^\circ$  structure has been observed with the STM<sup>6</sup> and by X-ray absorption spectroscopy.<sup>14</sup> In addition, these STM and X-ray studies also indicated that the Cu adlayer structure could be perturbed by the presence of Cl<sup>-</sup>. The open  $\sqrt{3}\times\sqrt{3}R30^\circ$  structure appears unique to the electrochemical environment, as metals evaporated onto metal surfaces in ultrahigh vacuum (UHV) typically exhibit close-packed behavior.<sup>15-17</sup>

The observation of structures that are not close packed in the Cu/Au(111) system makes it important to ascertain whether other adatoms and other electrolytes also give rise to open structures. One possible reason for the absence of  $1\times 1$  commensurate behavior in the Cu on Au(111) system is the gross mismatch between the lattice spacings of bulk Cu (0.256 nm) and bulk Au (0.288 nm). In this paper, we gauge the importance of this mismatch by examining structures arising from upd of Ag onto Au(111) where the bulk Ag lattice spacing is only 0.0004 nm less than that of gold. One might anticipate a greater likelihood of  $1\times 1$  commensurate Ag upd structures on the gold surface and, perhaps, less sensitivity to the electrolyte.

There have been several previous studies of the Ag/Au upd system since Rogers<sup>18,19</sup> discovered the upd effect in 1949. Morrison<sup>20</sup> and Lorenz et al.<sup>21</sup> demonstrated the occurrence of Ag upd on different surfaces. More recently, Bruckenstein and co-workers<sup>22</sup> utilized rotating ring disk electrode (RRDE) and

coulometric techniques to measure the amount of charge passed during monolayer formation and to comment on the kinetics of growth of the monolayer structure. Surface-extended X-ray absorption fine structure (SXAFS)<sup>23</sup> has been utilized to probe the upd monolayer structure, and these investigators found contributions from both the upd metal and oxygen from the electrolyte in the monolayer. Surface conductivity measurements have also been performed on this system.<sup>24</sup>

None of these studies were performed on well-characterized single-crystal electrodes, and thus definitive voltammetry of the Ag/Au(111) upd system is missing. In addition, the sensitivity of the upd monolayer to the electrolyte has also not been investigated. In this paper we correlate atom-resolved AFM images of Ag upd deposited on Au(111) with definitive voltammetry, and comment on the composition of the upd structures on the Au surface.

## 2. Experimental Section

AFM images were obtained with a Nanoscope II AFM<sup>25</sup> operating in constant force mode. Cantilevers<sup>25</sup> were microfabricated with integral Si<sub>3</sub>N<sub>4</sub> tips, and the force between tip and sample, optimized for each image, was nominally 10<sup>-9</sup> N. Image acquisition time was 10 s. Images were filtered for presentation by removing high-frequency components using software available with the Nanoscope II. Spacings and orientations were determined on unprocessed images.

Potential control was with a Bioanalytical Systems CV-1B, a BAS 100A, or a PAR 173/PAR 175 combination. A liquid cell made from glass held the electrolyte (~0.2 mL). A Ag wire, in contact with the electrolyte, served as the reference electrode, and all voltages are referred to this wire. Voltammetry obtained with this wire showed only small differences from that obtained in another cell with a saturated Hg/Hg<sub>2</sub>SO<sub>4</sub> reference. The counter electrode was a Au wire which was flame annealed prior to each use.

The working electrode (which was also the AFM substrate) was a 65-nm-thick Au film evaporated onto V2 grade mica with an exposed electrode area of 0.32 cm<sup>2</sup>.<sup>26</sup> The Au films were used within 24 h of their removal from the evaporator. We investigated the degree of order on these surfaces by checking their oxide formation voltammetry. Our Au(111) films yielded cyclic voltammograms (CV) very similar to that found with true Au(111) single crystals,<sup>27</sup> which suggests a high degree of order. Electrical connection to the working electrode was made with a wire which was not in contact with the electrolyte.

Silver solutions were prepared from reagent grade chemicals and Millipore-Q purified water. Perchloric acid was VWR ultrapure grade. The concentrations and makeup of the solutions were 1.0 mM AgClO<sub>4</sub> + 0.1 M HClO<sub>4</sub>, 0.77 mM Ag<sub>2</sub>SO<sub>4</sub> + 0.1 M H<sub>2</sub>SO<sub>4</sub>, 1.0 mM AgNO<sub>3</sub> + 0.1 M HNO<sub>3</sub>, 0.2 mM Ag<sub>2</sub>CO<sub>3</sub> + 0.1 M HClO<sub>4</sub>, and 0.1 mM Ag(C<sub>2</sub>H<sub>3</sub>COO) + 0.1 M Na(CH<sub>3</sub>COO) + 0.1 M CH<sub>3</sub>COOH. Solutions were not deoxygenated prior to use in the AFM experiments, but we observed no changes in the voltammetry with deoxygenation in other cells.

Experiments were performed by immersing the fresh Au on mica electrode at +300 mV and using slow (2 mV s<sup>-1</sup>) linear potential sweeps to move to potentials where AFM images were obtained. Care was taken to remain between the potentials for oxide formation (~0.7 V) and bulk deposition (0 V). Voltammetry in this region was stable for several hours, with exceptions noted below. AFM results showed no variation over the ~4-h time scale of the experiments as long as the potential limits above were maintained.

Coulometric measurements were made by both (a) potential step coulometry and (b) integration of voltammetric peak areas.<sup>28</sup> Both methods gave similar results. The values reported are the average of at

(6) (a) Magnussen, O. M.; Hotlos, J.; Nichols, R. J.; Kolb, D. M.; Behm, R. *J. Phys. Rev. Lett.* **1990**, *64*, 2929-2932. (b) Magnussen, O. M.; Hotlos, J.; Beitel, G.; Kolb, D. M.; Behm, R. *J. Vac. Sci. Technol.*, **B** **1991**, *9*, 969-975.

(7) Yau, S. L.; Vitus, C. M.; Schardt, B. C. *J. Am. Chem. Soc.* **1990**, *112*, 3677-3679.

(8) Szklarczyk, M.; Bockris, J. O'M. *J. Electrochem. Soc.* **1990**, *137*, 452-457.

(9) Manne, S.; Butt, H.-J.; Gould, S. A. C.; Hansma, P. K. *Appl. Phys. Lett.* **1990**, *56*, 1758-1759.

(10) Reviews: (a) Rugar, D.; Hansma, P. K. *Phys. Today* **1990**, *43*, 23-30. (b) Wickramasinghe, K. *Sci. Am.* **1989**, *261*(4), 98. (c) Sarid, D.; Elings, V. B. *J. Vac. Sci. Technol.*, **B** **1991**, *9*, 431-437. (d) Sarid, D. *Scanning Force Microscopy*; Oxford University: New York, 1991.

(11) Manne, S.; Hansma, P. K.; Massie, J.; Elings, V. B.; Gewirth, A. A. *Science* **1991**, *251*, 183-186.

(12) Manne, S.; Massie, J.; Elings, V. B.; Hansma, P. K.; Gewirth, A. A. *J. Vac. Sci. Technol.*, **B** **1991**, *9*, 950-954.

(13) Zei, M. S.; Qiao, G.; Lehmpfuhl, G.; Kolb, D. M. *Ber. Bunsen-Ges. Phys. Chem.* **1987**, *91*, 349-353.

(14) Tadjeddine, A.; Guay, D.; Ladouceur, M.; Tourillon, G. *Phys. Rev. Lett.* **1991**, *66*, 2235-2238.

(15) Chambliss, D. D.; Wilson, R. J. *J. Vac. Sci. Technol.*, **B** **1991**, *9*, 928-932.

(16) Dovek, M. M.; Lang, C. A.; Nogami, J.; Quate, C. F. *Phys. Rev. B* **1989**, *40*, 11973-11975.

(17) Somorjai, G. A. *Chemistry in Two Dimensions: Surfaces*; Cornell University: Ithaca, NY, 1981.

(18) Rogers, L. B.; Krause, D. P.; Griess, J. C.; Ehrlinger, D. B. *J. Electrochem. Soc.* **1949**, *95*, 33-46.

(19) Rogers, L. B. In *Electrochemistry, Past and Present*; Stock, J. T., Orna, M. V., Eds.; ACS Symposium Series 390; American Chemical Society: Washington, DC, 1989; pp 396-401.

(20) Sandoz, D. P.; Peekema, R. M.; Freund, H.; Morrison, C. F. *J. Electroanal. Chem. Interfacial Electrochem.* **1970**, *24*, 165-174.

(21) Lorenz, W. J.; Moutzisz, I.; Schmidt, E. *J. Electroanal. Chem. Interfacial Electrochem.* **1971**, *33*, 121-133.

(22) (a) Untereker, D. F.; Sherwood, W. G.; Bruckenstein, S. *J. Electrochem. Soc.* **1978**, *125*, 380-384. (b) Riedhammer, T. M.; Melnicki, L. S.; Bruckenstein, S. *Z. Phys. Chem. (Wiesbaden)* **1978**, *111*, 177-192. (c) Swathirajan, S.; Mizota, H.; Bruckenstein, S. *J. Phys. Chem.* **1982**, *86*, 2480. (d) Swathirajan, S.; Bruckenstein, S. *J. Electrochem. Soc.* **1982**, *129*, 1202-1210. (e) Swathirajan, S.; Bruckenstein, S. *J. Electroanal. Chem. Interfacial Electrochem.* **1983**, *146*, 137-155. (f) Melnicki, L. S. Ph.D. Thesis, State University of New York at Buffalo, September 1985.

(23) White, J. H.; Albarelli, M. J.; Abruna, H. D.; Blum, L.; Melroy, O. R.; Samant, M. G.; Borges, G. L.; Gordon, J. G. *J. Phys. Chem.* **1988**, *92*, 4432-4436.

(24) Romeo, F. M.; Tucceri, R. I.; Posadas, D. *Surf. Sci.* **1988**, *203*, 186-200.

(25) Digital Instruments, Inc., 6780 Cortona Dr., Santa Barbara, CA 93117.

(26) Evaporation parameters: pressure, <2 × 10<sup>-6</sup> Torr; mica temperature, 300 °C; evaporation rate, 0.1 nm/s.

(27) Angerstein-Kozłowska, H.; Conway, B. E.; Hamelin, A.; Stoicoviciu, L. *Electrochim. Acta* **1986**, *31*, 1051-1061.

(28) The measured current will be the sum of the double-layer charging current and the current due to upd. These are expected to be easily separable for the slow CV scan rates (<20 mV/s) used in these experiments. As a check, we measured the double-layer charging current by repeating the voltammetry in solutions not containing Ag.

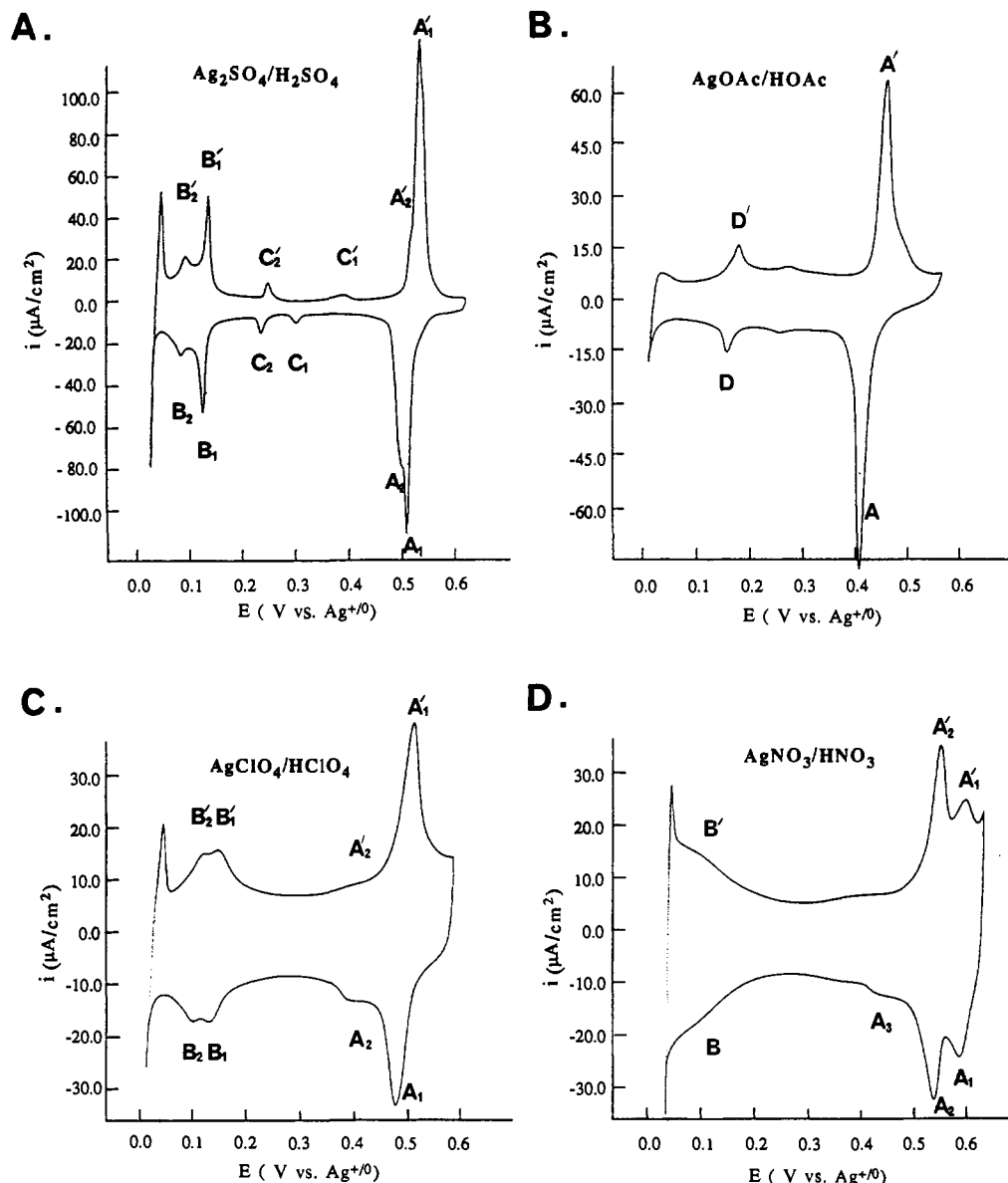


**Figure 1.** Cyclic voltammograms of Ag upd on Au(111) obtained in different electrolytes with adsorption (unprimed) and desorption (primed) peaks indicated: (A) sulfate electrolyte, (B) acetate electrolyte, (C) perchlorate electrolyte, (D) nitrate electrolyte. Scan rate was  $20 \text{ mV s}^{-1}$ .

least six different measurements utilizing fresh Au substrates each time.

### 3. Results

**3.1. Cyclic Voltammetry. 3.1.1. Sulfate Electrolyte.** Cyclic voltammetry for Ag upd on Au(111) in  $0.1 \text{ M H}_2\text{SO}_4$  is shown in Figure 1A. The voltammetry shows at least six sets of adsorption (unprimed) and desorption (primed) peaks corresponding to several distinct processes occurring in the underpotential region. This voltammetry agrees qualitatively with that given by Lorenz et al.,<sup>21</sup> but differs in the number and sharpness of peaks. This may be due to our use of a nearly single crystal surface relative to the polycrystalline materials used in prior experimentation and to our slow scan rates ( $20 \text{ mV s}^{-1}$ ).

Two main peaks are seen in this voltammetry. At  $507 \pm 3 \text{ mV}$  (peak  $A_1$ ) the first deposition of Ag onto Au(111) occurs. This peak is split, with peak  $A_2$  occurring at  $490 \text{ mV}$ . The potential difference between corresponding stripping peaks  $A_1'$  and  $A_2'$  was less than  $30 \text{ mV}$ . The width of these peaks ( $<10 \text{ mV}$ ) compares well with that found for upd peaks in other single-crystal systems.<sup>29</sup> Prior to bulk deposition, another series of peaks ( $B_1$  and  $B_2$  for deposition,  $B_1'$  and  $B_2'$  for stripping) at  $117 \pm 12$  and  $79 \pm 7 \text{ mV}$  occur, corresponding to another upd process involving the Ag

monolayer. CVs run over the entire potential range in solutions not containing Ag exhibited only double-layer charging currents and no peaks. Two other peaks are seen between the larger bands already discussed. These smaller features, labeled  $C_1$  and  $C_2$  (and  $C_1'$  and  $C_2'$ ), are somewhat broader and also not as reversible as the other main features. The potentials for each peak and charge passed after subtraction of double-layer charging are given in Table I.

This voltammetry was quite stable and reversible and persisted over many cycles lasting several ( $>4$ ) h. This suggests that alloy formation between Ag and Au in the upd potential region does not occur, a result also suggested by RRDE measurements.<sup>22</sup> If the potential was moved either into the gold oxide region (potentials more positive than  $+700 \text{ mV}$ ) or far into the bulk silver region (potentials more negative than  $-50 \text{ mV}$ ), then the voltammetry changed substantially with loss of the sharp upd features and significant peak shifts. We attribute these changes to modification of the Au(111) surface occurring with either of these treatments. Chidsey,<sup>30</sup> for example, has shown that oxide formation on Au(111) surfaces results in pitting and roughening of the surface. Substantial potential excursions into the bulk de-

(29) Schultze, J. W.; Dickertmann, D. *Surf. Sci.* **1976**, *54*, 489–505.

(30) Trevor, D. J.; Chidsey, C. E. D.; Loiacono, D. N. *Phys. Rev. Lett.* **1989**, *62*, 929–932.

**Table I.** Peak Positions and Charges for Ag Upd on Au(111) in Different Electrolytes

electrolyte	peak	potential (mV vs Ag <sup>+0</sup> )	charge density ( $\mu\text{C}/\text{cm}^2$ )
sulfate	A <sub>1</sub> , A <sub>2</sub>	507 ± 3	154 ± 7
	C <sub>1</sub>	296 ± 2	
	C <sub>2</sub>	235–250	
	B <sub>1</sub> , B <sub>2</sub>	117 ± 12, 79 ± 7	69 ± 8
	A <sub>1</sub> ' , A <sub>2</sub> '	530 ± 3	150 ± 12
	C <sub>1</sub> '	361–389	
	C <sub>2</sub> '	249–270	
	B <sub>1</sub> ' , B <sub>2</sub> '	133 ± 5, 93 ± 5	75 ± 15
nitrate	A <sub>1</sub> , A <sub>2</sub> , A <sub>3</sub>	581 ± 6, 541 ± 1	101 ± 9
	B	a	56 ± 10
	A <sub>1</sub> ' , A <sub>2</sub> '	607 ± 2, 557 ± 3	112 ± 12
	B'	a	56 ± 9
perchlorate	A <sub>1</sub> , A <sub>2</sub>	471 ± 5	99 ± 10
	B <sub>1</sub> , B <sub>2</sub>	107 ± 6	40 ± 7
	A <sub>1</sub> ' , A <sub>2</sub> '	513 ± 5	100 ± 10
	B <sub>1</sub> ' , B <sub>2</sub> '	130 ± 7	49 ± 9
acetate	A	405 ± 4	144 ± 8
	D	160 ± 5	b
	A'	451 ± 5	127 ± 12
	D'	175 ± 5	b

<sup>a</sup>Unable to measure accurately. <sup>b</sup>This peak does not correspond to a upd process; see text.

position region leads to alloy formation which requires significant overpotentials in stripping. This again leads to roughening of the electrode surface<sup>31</sup> and broader upd peaks with altered positions.

**3.1.2. Other Electrolytes.** The overall shape of the voltammetry in nitrate (Figure 1D) and perchlorate (Figure 1C) electrolytes is qualitatively similar to that obtained in sulfuric acid. In each, a relatively sharp upd feature around 500 mV (peaks A and A') is followed by broader and less intense features between +100 and +200 mV (peaks B and B'). Neither of these electrolytes gave the very sharp features found in sulfate. However, if a drop of sulfuric acid was added to these solutions, then the characteristic sulfate voltammetry was recovered. We thus feel that the differences in voltammetry cannot be ascribed to differences in surface preparation or to adventitious contamination of the other electrolytes.

CVs obtained in nitric and sulfuric acid were quite stable and reproducible over a period of several (>4) h. This was not the case for voltammetry in perchloric acid. In this electrolyte, we found that peak splittings in the features between 75 and 150 mV (peaks B<sub>1</sub> and B<sub>2</sub>) could not always be observed. In addition, the shoulder just positive of the main features at 490 mV varied in intensity relative to the main peak. The variation in voltammetry in perchlorate may reflect greater sensitivity of this system to surface structure or to small amounts of contaminants. The other electrolytes studied are thought to adsorb on the Au(111) surface, while this is probably not the case for perchlorate. The lack of specific adsorption may make the voltammetry in the perchlorate system more sensitive.

In acetate electrolyte, we saw (Figure 1B) two sets of peaks (A and A', D and D') positive of the bulk deposition region. While peaks A and A' are associated with the Ag upd process, and are not found in solutions lacking Ag, peaks D and D' appear to be associated with the acetate as they occur even in solutions lacking silver ion. The AgOAc system is thus unique relative to the other electrolytes considered in this paper in that only one set of upd peaks occur. In the other systems studied, two main sets of upd peaks are found prior to bulk deposition. In the next section, we will see that this change in voltammetry has a specific structural consequence.

**3.2. AFM Images.** Long-range scans of the Au(111) surface revealed large terraces similar to those described by Chidsey<sup>32</sup> and Putnam et al.<sup>33</sup> The amount of disordered area between

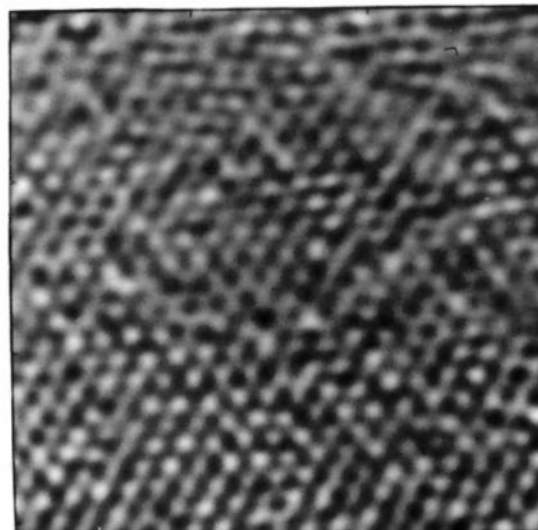


**Figure 2.** 5 × 5 nm image of an Au(111) surface in solution obtained positive of the first upd peaks. Atom-atom spacing is 0.29 nm.

terraces was small, corresponding to ca. 20% of the total surface area.

**3.2.1. Sulfate Electrolyte.** In sulfuric acid electrolyte, several different structures were observed at different potentials, corresponding to different stages of the upd process. At potentials positive of the first upd peak, AFM images (Figure 2) in every electrolyte studied exhibited atomic resolution with an atom-atom spacing of  $0.29 \pm 0.02$  nm corresponding to the bare Au(111) surface. The apparent corrugation in this, and in the other images reported in this work, ranged between 0.04 and 0.08 nm, depending upon the particular tip used. In contrast to the situation in the Cu/Au(111) systems reported previously,<sup>11</sup> this corrugation did not exhibit long-term stability, most likely due to nascent oxide formation (the Ag<sup>+0</sup> couple occurs some 460 mV more positive than the Cu<sup>2+/0</sup> pair, and oxide formation begins at ca. +700/mV).<sup>34</sup> There is strong radiochemical evidence<sup>35,36</sup> that sulfate associates with the surface at these potentials, which are substantially positive of the potential of zero charge (pzc).<sup>37</sup> However, scanning just negative of potentials where oxide is formed (+650 mV) never revealed any atomic resolution structures other than that from the Au(111) lattice even when extremely weak (<10<sup>-10</sup> N) scanning forces were used. STM images taken at positive potentials in sulfate also exhibit only the Au(111) corrugation.<sup>6,38</sup> The inability of either technique to image sulfate adsorbed onto the Au(111) surface may mean that the sulfate is very weakly adsorbed and the tip-surface interaction is strong enough to sweep the anion away.

After cycling through the first monolayer deposition peaks A<sub>1</sub> and A<sub>2</sub> to potentials between 500 and 240 mV (between peaks A<sub>2</sub> and C<sub>2</sub> in Figure 1A), we observed images (Figure 3A) with atom-atom spacings of  $0.43 \pm 0.03$  and  $0.86 \pm 0.03$  nm. The atoms exhibited a hexagonal pattern, with a  $0 \pm 10^\circ$  rotation relative to the atomic orientation observed in Au(111) lattice images taken immediately (30 s) prior to sweeping the potential through the most anodic upd peaks. We have ascertained previously<sup>12</sup> that drift rates in the AFM are low enough to ensure

(33) Putnam, A.; Blackford, B. L.; Jericho, M. H.; Wantanabe, M. O. *Surf. Sci.* **1989**, *217*, 276–288.

(34) Bard, A. J.; Faulkner, L. R. *Electrochemical Methods*; John Wiley: New York, 1980.

(35) (a) Horanyi, G.; Rizmayer, E. M.; Joo, P. *J. Electroanal. Chem. Interfacial Electrochem.* **1983**, *152*, 211–222. (b) Horanyi, G.; Rizmayer, E. M.; Joo, P. *J. Electroanal. Chem. Interfacial Electrochem.* **1983**, *154*, 281–286.

(36) Zelenay, P.; Rice-Jackson, L. M.; Wiekowski, A. *J. Electroanal. Chem. Interfacial Electrochem.* **1990**, *283*, 389–401.

(37) Kolb, D. M.; Schneider, J. *Electrochim. Acta* **1986**, *31*, 929–936.

(38) Hachiyu, T.; Honbo, H.; Itaya, K. *J. Electroanal. Chem. Interfacial Electrochem.*, in press.

(31) Oppenheim, I. C.; Trevor, D. J.; Chidsey, C. E. D.; Trevor, P. L.; Sieradzki, K. *Science*, submitted for publication.

(32) Chidsey, C. E. D.; Loiacono, D. N.; Sleanor, T.; Takahara, S. *Surf. Sci.* **1988**, *200*, 45–66.

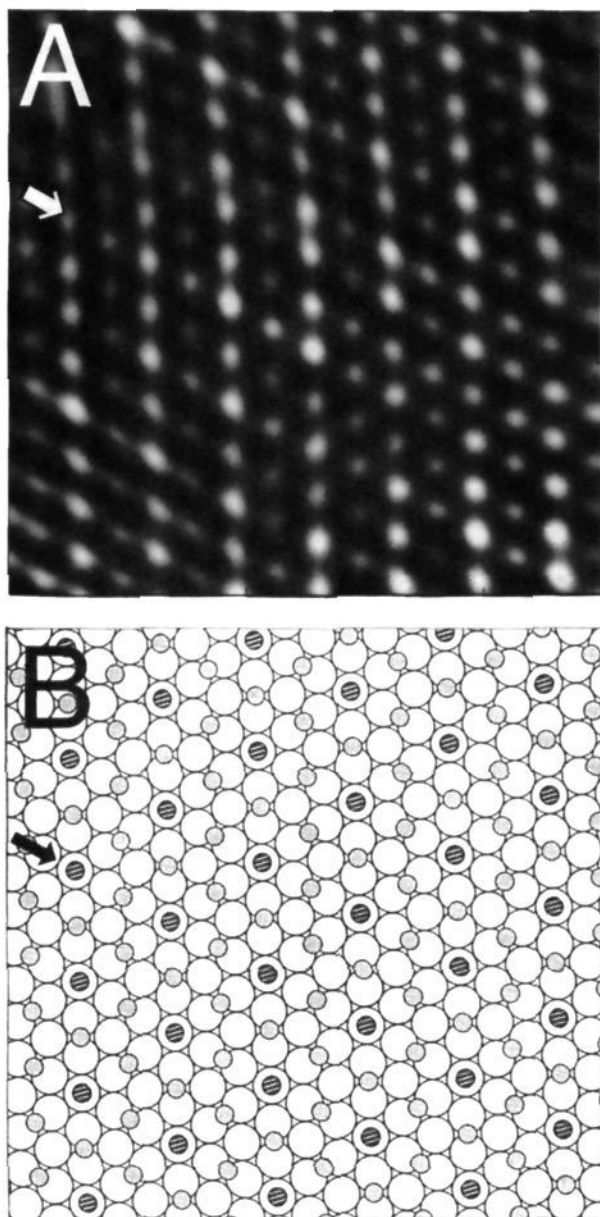


**Figure 3.** (A)  $5 \times 5$  nm image of the first upd monolayer of Ag on Au(111) in 0.1 M  $\text{H}_2\text{SO}_4$  obtained at +420 mV vs  $\text{Ag}^{+}/0$ . The arrow indicates rows of atoms in alternating atop and bridging sites. (B) Schematic of the  $3 \times 3$  structure of Ag on Au(111) in sulfate. Small circles represent Ag, while large circles represent the Au(111) surface. Black striped circles are Ag atoms in atop sites, and lighter small circles represent Ag atoms in bridging sites. The arrow indicates rows of atoms in alternating atop and bridging sites.

that both sets of images were obtained in approximately the same location. Two-dimensional Fourier transforms of these images yielded two sets of six concentric spots at spacings corresponding to the distances given above which were not rotated relative to each other. This is equivalent to a  $3 \times 3$  overlayer (Figure 3B) and corresponds to a 44% packing density on the surface. This result is consistent with RRDE experiments<sup>22c</sup> for Ag upd on polycrystalline Au which gave approximately 50% surface coverage at these potentials. It is thus likely that all of the features in Figure 3A correspond to Ag adatoms rather than a mixture of Ag and coadsorbed electrolyte on the Au(111) surface.

In Figure 3B, we have placed the adatoms in atop sites and 2-fold bridging sites. Another possible arrangement, related to that shown in Figure 3B by a translation, would have adatoms in bridging and 3-fold hollow sites. In both cases, a consequence of these two different sites is that a row structure exhibiting

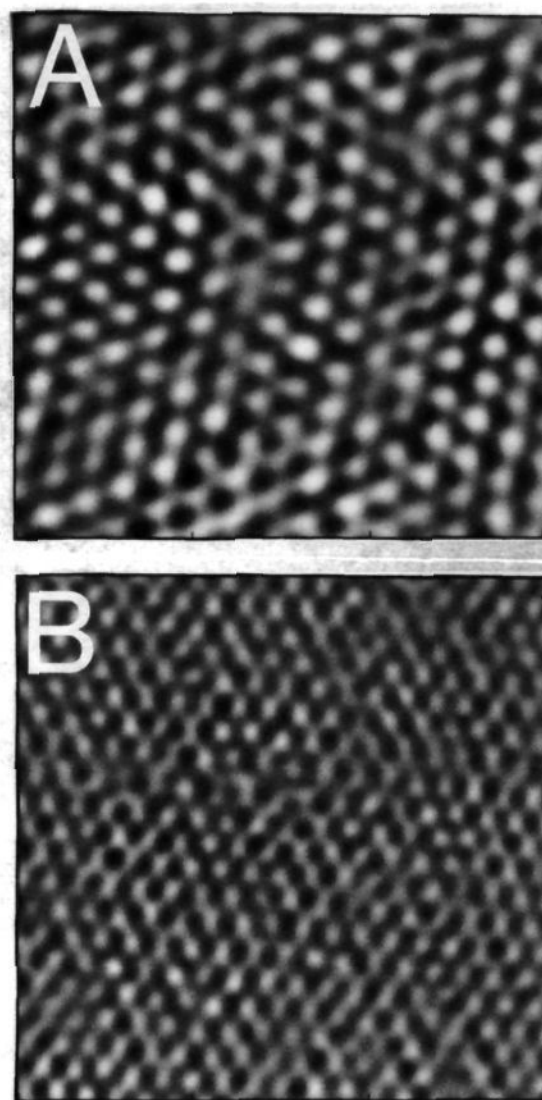


**Figure 4.** (A)  $5 \times 5$  nm AFM image of Ag on Au(111) in sulfate obtained at a potential of +50 mV, just positive of bulk deposition. The atom-atom spacing is 0.43 nm. (B)  $5 \times 5$  nm AFM image of Ag(111) bulk deposited onto Au(111). The atom-atom spacing is 0.29 nm.

alternating higher and lower rows should obtain, and indeed, in Figure 3A this is exactly what is observed. Because we observe height modulation in the row of higher atoms, marked with an arrow in Figure 3A, we favor the structure which has silver atoms in atop sites.<sup>39</sup> The other structure would require modulation in the row of lower atoms, and we do not observe this in the image. In Figure 3A, the vertical modulation between rows is  $0.05 \pm 0.02$  nm, which is on the correct order for the height difference between atoms on atop sites and atoms in 2-fold bridging sites (calculated 0.039 nm).

Between points  $C_2$  and  $B_2$  (between 240 and 100 mV) in the sulfate voltammetry shown in Figure 1A, no clear atom-resolved corrugation was found. The lack of corrugation in this potential region is not due to intrinsic imaging problems, as sweeping to potentials outside of this range again affords atomic resolution in the same location. Our inability to resolve atoms may thus be ascribed to some process which causes the surface to disorder or to an unstable surface which is undergoing some type of rapid

(39) Note that the modulation in Figure 3A is clear for only two of the three directions in the hexagonal lattice and is much fainter in the vertical rows which are perpendicular to the scan direction. However, rotating the scan direction by  $60^\circ$  yielded images identical to the one shown. Thus, the faint modulation in the vertical rows is attributed to a scan artifact.

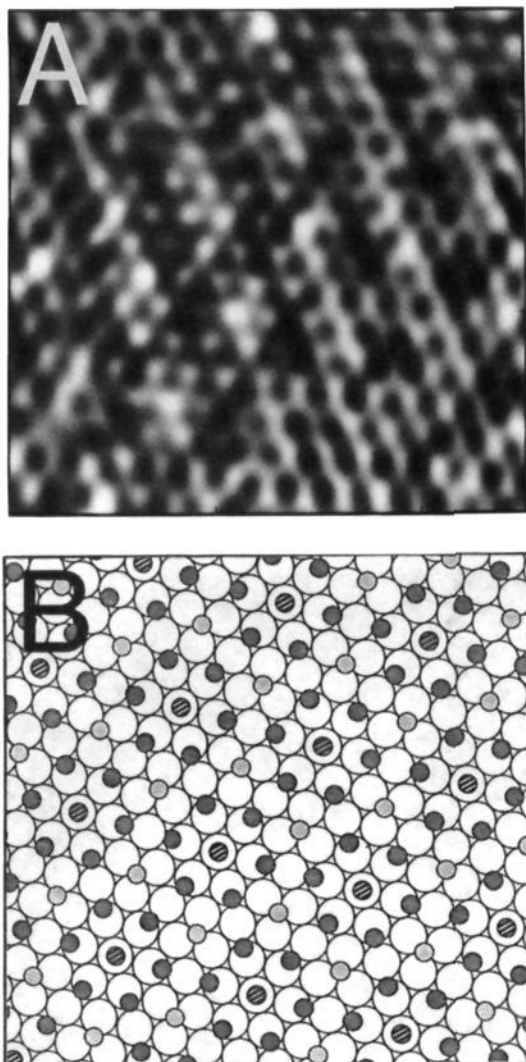


**Figure 5.** (A)  $5 \times 5$  nm AFM image of Ag on Au(111) in nitrate obtained at +460 mV vs  $\text{Ag}^{+/0}$ . (B) Schematic of the  $4 \times 4$  lattice formed by upd of Ag on Au(111) in nitric acid. Small circles represent Ag, while large circles represent the Au(111) surface. Black striped circles are Ag atoms in atop sites, light small circles represent Ag atoms in 3-fold hollow sites, and dark small circles show Ag atoms in bridging sites.

exchange process with the electrolyte.

At potentials negative of  $B_2$  but before the bulk region, images like that shown in Figure 4A were obtained. These images also exhibited the  $0.43 \pm 0.02$  nm atom–atom distance found in the  $3 \times 3$  structure at more positive potentials. However, we were not able to observe the larger, 0.86-nm spacing that was seen at the more positive potentials. We conclude that at this potential the upd monolayer is open but incommensurate. The monolayer is not close packed and still retains features associated with the  $3 \times 3$  lattice observed at potentials over 400 mV more positive. The voltammetric peaks  $B_1$  and  $B_2$  are thus ascribed to a commensurate to incommensurate transition occurring in the Ag upd lattice as more Ag is deposited. While specific confirmation of this feature will have to await more detailed synchrotron studies,<sup>40</sup> to our knowledge this represents the first observation of this type of transition in a upd system.

Reversing the potential scan direction strips the upd Ag and reexposes the bare Au(111) surface. The voltammetry is reversible, and we observed the same structural features in anodic current as were observed cathodically.

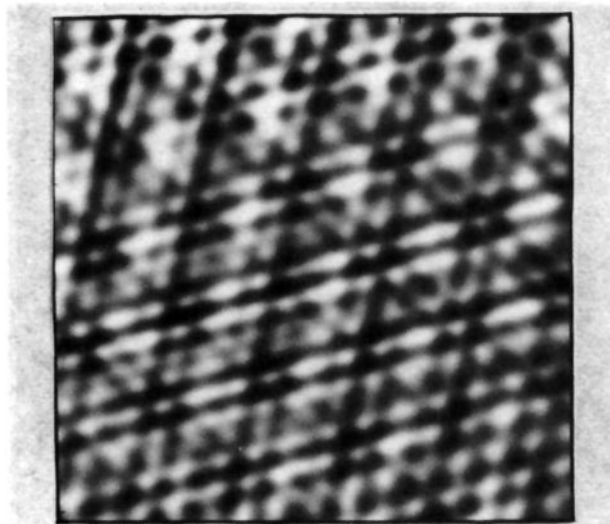


**Figure 6.**  $5 \times 5$  nm AFM image of Ag upd on Au(111) in perchloric acid taken at +445 mV vs  $\text{Ag}^{+/0}$ . Short atom–atom spacings of 0.29 nm and long spacings of 0.40 nm are observed.

Finally, sweeping the potential to  $-10$  mV instead of stripping the upd Ag leads to the initiation of bulk deposition and gives rise to a close-packed structure with a  $0.29 \pm 0.02$  nm spacing (Figure 4B) which we associate with bulk Ag(111) on the surface. Ag thus becomes yet another bulk metal that affords atomic resolution with the AFM in an electrochemical environment.

**3.2.2. Nitrate Electrolyte.** In nitrate-containing electrolytes, we again observed the Au(111) surface with its characteristic 0.29-nm corrugation at potentials positive of the first deposition peak  $A_1$  in Figure 1D. Cycling past these peaks into the potential region between  $A_3$  and B gives rise to images (Figure 5A) which were substantially different from those observed in sulfuric acid. These images exhibit hexagonal structure, short atom–atom spacings of  $0.38 \pm 0.03$  nm, and longer distance row spacings of  $1.12 \pm 0.04$  nm. There was no rotation relative to the underlying Au(111) surface. These images were not as well resolved as those obtained in sulfate electrolyte. However, the only structure which satisfies the above spacings is a  $4 \times 4$  lattice, which is shown in Figure 5B. The  $4 \times 4$  structure implies 56% surface coverage which is again consistent with RRDE results in nitrate electrolyte.<sup>22f</sup> The  $4 \times 4$  structure again has atoms in different types of sites on the Au(111) surface. An atom in an atop site is surrounded at short distance (0.38 nm) by six atoms in 2-fold bridging sites. At longer distance (0.66 nm) the central atom is surrounded by six others in 3-fold hollow sites. The arrangement of atoms requires modulation of the row structure on the electrode surface, and in Figure 5A, this modulation gives rise to the larger 1.12-nm spacings seen.

Cycling negative of point B in Figure 1D did not give rise to any other atom-resolved images on this surface until the onset of bulk deposition. The electrochemistry in this potential region showed a broad current background even at slow ( $<20$  mV/s) scan rates, which could be related to fluxional processes occurring on the electrode surface.

**3.2.3. Perchlorate Electrolyte.** In perchlorate electrolyte, yet another structure of Ag on Au(111) was observed. In these images (Figure 6), taken at potentials between points  $A_2$  and  $B_1$  in Figure 1C, we found atomic resolution images with short atom–atom spacings of  $0.29 \pm 0.02$  nm, and longer distance spacings of  $0.40 \pm 0.01$  nm every two rows. This 0.40-nm spacing is of the correct magnitude for a  $(\sqrt{7} \times \sqrt{7})R19.1^\circ$  overlayer structure where a 0.38-nm spacing would be expected. However, we would also expect a modulation of atoms in this structure similar to that found in the  $4 \times 4$  (nitrate) and  $3 \times 3$  (sulfate) structures discussed above. We never observed this modulation, and could not definitively ascertain the rotation of this lattice relative to the underlying Au(111) surface. This structure must thus remain unassigned. However, we could estimate the packing density on

(40) Melroy, O. R.; Toney, M. F.; Borges, G. L.; Samant, M. G.; Kortright, J. B.; Ross, P. N.; Blum, L. *Phys. Rev. B* 1988, 38, 10962–10965.

**Table II.** Comparison of AFM- and Electrochemically-Derived Coverage for Ag Upd on Au(111) in Different Electrolytes

electrolyte	structure (AFM)	% coverage (AFM)	% coverage <sup>a</sup> (coulometry)	radius <sup>b</sup> (nm)	pK <sub>a</sub> <sup>c</sup>
sulfate	3 × 3	44	68 ± 4	0.244	-3 (pK <sub>a1</sub> )
nitrate	4 × 4	56	50 ± 5	0.165	-1.6
perchlorate	<i>d</i>	65 ± 10 <sup>e</sup>	45 ± 6	0.226	-8
acetate	close-packed	100	62 ± 6	0.148	4.8

<sup>a</sup> Obtained by averaging cathodic and anodic charges for the most positive upd and ups peaks. <sup>b</sup> Huheey, H. E. *Inorganic Chemistry*, 3rd ed.; Harper & Row: New York, 1983; p 78. <sup>c</sup> Gordon, A. J.; Ford, R. A. *The Chemist's Companion: a Handbook of Practical Data, Techniques, and References*; John Wiley & Sons: New York, 1972; pp 58-59. <sup>d</sup> Structure not solved; see text. <sup>e</sup> Estimated by inspection.

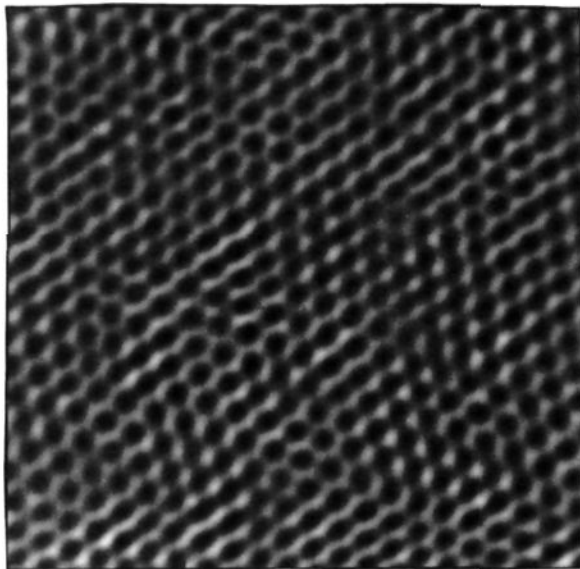


**Figure 7.** 5 × 5 nm AFM image of Ag upd on Au(111) in acetic acid obtained +400 mV vs Ag<sup>+/0</sup>. Atom-atom distance is 0.29 nm.

the surface by counting the number of atoms in a given area. In perchlorate we obtained a packing density of 65 ± 10%.

More negative of peaks B<sub>1</sub> and B<sub>2</sub>, but positive of the bulk potential region, we again observed an open lattice structure. This lattice exhibited only the 0.40-nm spacing, but no modulation was resolved. However, it is clear that the structure is not close packed.

Cycling into the bulk potential region again gave a close-packed Ag(111) lattice with the expected 0.29-nm atom-atom spacing.

**3.2.4. Acetate Electrolyte.** The last system studied was Ag upd in acetic acid. In contrast to the other electrolytes investigated, the voltammetry exhibited only one peak attributable to Ag upd. AFM images (Figure 7) obtained in the potential region between points A and D in Figure 1B (between +450 and +150 mV) exhibited only a close-packed hexagonal structure with an atom-atom spacing of 0.29 ± 0.01 nm. The lattice appeared unrotated relative to the images of the Au(111) surface obtained at potentials positive of the upd band A. This is equivalent to a close-packed commensurate overlayer of Ag on Au(111). Thus, only in acetic acid does the anticipated close-packed structure obtain. Cycling negative, past point D, the images became unclear. We did not observe any other structure in this system until the onset of bulk deposition where we again saw the Ag(111) lattice.

#### 4. Discussion

In UHV environments, Ag grows onto Au(111) via an aggregation mechanism resulting in a close-packed incommensurate overlayer structure.<sup>15,16</sup> This structure is the result of attractive forces between Ag adatoms. In electrochemical environments, the observation of open structures implies that the forces between adatoms are repulsive, a point which has been emphasized previously.<sup>6</sup> The differing AFM images in different electrolytes demonstrate that the electrolyte plays a central role in determining the structure of the first Ag monolayer on Au(111) surfaces. Clearly this suggests strong participation of the electrolyte in the upd monolayer and that the electrolyte contributes to the repulsive

forces making the open structures observed. These repulsive forces could arise either from repulsions between the anions themselves or from partial charges remaining on the Ag adatoms.

Strong participation of the electrolyte in the upd monolayer has been suggested by a variety of studies. Radiochemical studies of Ag upd on Au surfaces indicated adsorption of sulfuric acid electrolyte onto Au(111) at potentials positive to the upd peak.<sup>35</sup> In addition, X-ray studies of both Cu<sup>41</sup> and Ag<sup>23</sup> upd found strong participation from O of sulfate and perchlorate electrolytes in the first coordination sphere of the adatom. Ag upd occurs approximately 300 mV positive of the Au(111) potential of zero charge, and it is not surprising that substantial electrolyte association with the surface has occurred.

**4.1. Discussion of the Different Structures.** The different electrolytes must interact differently both with the electrode surface and with the Ag adatom in order to produce the different structures observed. In Table II the different structures are compared with the pK<sub>a</sub> and size of the different acids used.

**4.1.1. Sulfate.** In sulfate, the Ag upd overlayer exhibits a 3 × 3 lattice implying 44% surface coverage by Ag. The open structure is presumably stabilized by participation of bisulfate in the upd lattice. There are three possible ways bisulfate could participate in the upd structure. First, the bisulfate could be adsorbed in the interstices of the 3 × 3 lattice. Second, it could be adsorbed directly atop the Ag adatoms in a 1:1, 2:1, or other ordered arrangement. Third, the bisulfate could be disordered above the Ag adlattice.

In the first possibility, the atom-atom spacing in the 3 × 3 lattice is 0.43 nm which gives rise to interstitial holes with a diameter of 0.21 nm, assuming a Ag atom diameter of 0.28 nm. However, the diameter of the bisulfate molecule is 0.488 nm, and so is much larger than the interstitial hole space. Both ordered and disordered overlayers of sulfate above the Ag adatoms, the second and third possibilities, would be consistent with the AFM images shown above. An ordered structure of bisulfate on top of the Ag adatoms also would be consistent with X-ray measurements on both the Cu/sulfate/Au(111)<sup>41</sup> and Ag/sulfate/Au(111)<sup>23</sup> systems, where participation of an O from the electrolyte was found in the first coordination sphere of the adatom. Other researchers have also found ordered arrays of sulfate on Au<sup>42</sup> and other emersed electrode surfaces.<sup>43</sup> The X-ray results<sup>23,41</sup> suggested a 1:1 coordination of anion atop the adatom. While that possibility is consistent with the AFM images, other arrangements cannot be excluded.

We note that the 3 × 3 adlattice found with Ag in sulfate is somewhat less open than the √3 × √3R30° structure (33% coverage) found in the same electrolyte during Cu upd.<sup>6,11</sup> The different structures found with the different metals in sulfate thus cannot relate entirely to the different sizes of the metal adatom, as the larger size of Ag (0.29 nm) relative to Cu (0.26 nm) would suggest a less, not more, densely packed surface. The more open structure in Cu may reflect a greater partial charge on this metal relative to Ag as recent X-ray absorption work<sup>14</sup> has found a

(41) Melroy, O. R.; Samant, M. G.; Borges, G. L.; Gordon, J. G.; Blum, L.; White, J. H.; Albarelli, M. J.; McMillan, M.; Abruna, H. D. *Langmuir* 1988, 4, 728-732.

(42) (a) Zei, M. S.; Scherson, D.; Lehmpfuhl, G.; Kolb, D. M. *J. Electroanal. Chem. Interfacial Electrochem.* 1987, 229, 99-105. (b) Zei, M. S.; Weick, D. *Surf. Sci.* 1989, 208, 425-440.

(43) Ehlers, C. B.; Stickney, J. L. *Surf. Sci.* 1990, 239, 85-102 and references therein.

charge of +1 on the Cu while the charge on upd Ag must be less than this.

**4.1.2. Nitrate, Carbonate, and Acetate.** Nitrate, carbonate,<sup>44</sup> and acetate electrolytes all give rise to higher packing densities of Ag on the Au(111) surface. In nitric acid electrolyte, for example, the Ag overlayer occupies 12% more of the surface than the overlayer in sulfate. These two electrolytes have almost the same  $pK_a$  (-2 for sulfate -1.6 for nitrate), suggesting similar degrees of association with the Ag, but the radius of nitrate (0.165 nm) is substantially smaller than that of sulfate (0.244 nm). Carbonate has a much higher  $pK_a$  relative to nitric acid, but an identical radius, and gives rise to the same (4 × 4) upd structure of Ag. Finally, acetate has a small radius (0.148 nm), and yields a close-packed Ag structure.

While there are certainly interactions between the anion and water at the solid-liquid interface which make our knowledge of electrolyte size uncertain, the trend given in Table II does suggest that electrolyte size is one important factor in overlayer structure determination. The increase in electrolyte size leads to increased repulsive forces which serve to open the upd structure. While other interactions are certainly also important in determining overlayer structure, changing electrolyte size from larger to smaller leads to overlayer structures exhibiting higher and higher packing densities in the Ag on Au(111) upd system studied here.

**4.1.3. Perchlorate.** Images in perchlorate revealed a packing density of  $65 \pm 10\%$  of Ag on the Au(111) surface. Perchlorate has a size intermediate to that of nitrate and sulfate, but it appears that the packing density is similar to that found in nitrate. This packing density may reflect the lack of specific adsorption of perchlorate onto the Au(111) surface. Both sulfate and nitrate, considered above, are thought to strongly adsorb onto Au at the Ag upd potential. Alternatively, Stimming<sup>45</sup> has suggested that perchlorate adopts a clathrasil structure near the electrode surface and is not strongly adsorbed. This clathrasil lattice may play a significant role in determining the structure of Ag upd on Au(111) in perchloric acid.

**4.2. Correlation of Monolayer Structure with Charge.** Determination of the structure of the upd monolayer allows comparison of the AFM-derived coverage with that predicted by coulometric measurements. In Table II, this comparison is given for the four electrolytes exhibiting stable voltammetry studied here. In obtaining the coverage, we assumed that  $220 \mu\text{C}/\text{cm}^2$  were required for one-monolayer coverage of Ag. We also assume here that the local surface structure obtained with the AFM is representative of the full surface coverage. This latter assumption is justified on two grounds. First, the coverages found with the AFM agree generally with independent RRDE measurements<sup>22</sup> on polycrystalline surfaces. Second, the structures reported above appeared throughout the  $1 \mu\text{m}^2$  scan area available with our AFM. If other structures existed on the surface, it is likely that we would observe them over an area this large. From Table II, it is clear that, with the exception of nitrate, there are substantial inconsistencies between the charge passed and the surface coverage found.

In perchlorate and acetate electrolytes, the AFM gives surface coverages of 65% and 100%, respectively. However, only 60% (acetate) to 70% (perchlorate) of the charge required to form this monolayer is passed through the working electrode. This must mean that some of the charge required to reduce the  $\text{Ag}^+$  in solution comes from the electrolyte. In turn, this implies that there exists some kind of covalent interaction between the electrolyte

and the Ag adatom which leaves the adatom in a formal oxidation state which is greater than 0 but less than 1. Abruna<sup>46</sup> and Tadjeddine<sup>14</sup> have also found partial discharge of upd adatoms in complexing electrolytes. The trend observed in this work between acetate and perchlorate relative to this insufficient charge (missing 38% and 31%, respectively) is consistent with the anticipated trend in covalent delocalization between the two ligands. Perchlorate is a harder ligand than acetate, and perchlorate complexes should thus be more ionic than those with acetate ligands. While the comparison between complexes and surfaces is not strictly valid, this does support the idea that some degree of charge transfer between the Ag adatom and the electrolyte is occurring, requiring the electrolyte to be in some way bound to the Ag. This in turn is consistent with our finding of a size correlation between the electrolyte and the AFM-observed surface structure.

In sulfate and nitrate electrolytes, we find either no discrepancy between structure and charge or else that too much charge is passed. The electrochemistry predicts a surface coverage in sulfate of  $68 \pm 4\%$  of a monolayer while the real coverage as determined by the AFM is only 44%. In nitrate the AFM and electrochemical results are both consistent with 56% surface coverage by the Ag adatom. The discrepancy in Cu upd systems between coverage and electrochemical charge was also noted by Kolb,<sup>6</sup> and has been found to vary as a function of coverage by Goodman.<sup>47</sup> In the Cu systems, the correlation between charge and coverage is potentially complicated by the presence of an additional oxidation state for the Cu in solution, which may contribute to the reduction current. No such possibility exists, however, for Ag systems, yet the charge discrepancy remains. Clearly, the electrolyte must contribute to the current, perhaps through an anion discharge mechanism,<sup>6</sup> but the source of additional reduction equivalents remains uncertain.

## 5. Conclusions

We have shown that different upd structures of Ag on Au(111) occur in different electrolytes. In electrolytes which can complex to the Ag, we find a correlation between packing density observed with the AFM and electrolyte size, with larger electrolytes yielding more open structures. This variability with electrolyte is ascribed to differing repulsive interactions arising from anions coadsorbed with the metal adatom. These monolayers thus represent unique inorganic systems where adatom bonding to the electrolyte as well as the surface must be considered. This bonding to the electrolyte complicates substantially correlations between charge and structure, and structural determinations based on charge alone are likely to be incorrect. Further insight into these systems will originate not only from AFM and STM measurements of surface structure on other crystal faces, but also from detailed coulometric, radiochemical, and spectroscopic studies, and this work is in progress.

**Acknowledgment.** We thank Dr. Dennis Trevor for helpful suggestions for preparing Au films on mica. C.-H.C. acknowledges a University of Illinois Fellowship in Chemistry. S.M.V. acknowledges a REU summer fellowship sponsored by the NSF and the Materials Research Lab at the University of Illinois. A.A.G. acknowledges a Presidential Young Investigator award (CHE-90-57953) with matching funds generously provided by Digital Instruments, Inc. This work was funded by the NSF (Grant DMR-89-20538) through the Materials Research Laboratory at the University of Illinois.

**Registry No.** Ag, 7440-22-4; Au, 7440-57-5;  $\text{HClO}_4$ , 7601-90-3;  $\text{H}_2\text{SO}_4$ , 7664-93-9;  $\text{HNO}_3$ , 7697-37-2;  $\text{CH}_3\text{COOH}$ , 64-19-7;  $\text{Na}(\text{CH}_3\text{COO})$ , 127-09-3;  $\text{CO}_3^{2-}$ , 3812-32-6;  $\text{CO}_2$ , 124-38-9.

(44) Images in carbonate electrolyte initially showed very clear  $4 \times 4$  structures at potentials just negative of the first upd peak. However, the voltammetry was unstable over time due to the formation of  $\text{CO}_2$ . As the voltammetry changed the images became less clear and the structure uncertain.

(45) Cappadonia, M.; Stimming, U. *J. Electroanal. Chem. Interfacial Electrochem.* **1991**, *300*, 235-248.

(46) White, J. H.; Abruna, H. D. *J. Phys. Chem.* **1990**, *94*, 894-900.  
(47) Leung, L.-W. H.; Gregg, T. W.; Goodman, D. W. *J. Am. Chem. Soc.*, in press.